Dysregulation of fatty acid synthesis and glycolysis in non-Hodgkin lymphoma

Aadra P. Bhatt[a,b], Sarah R. Jacobs[a,b], Alex J. Freemerman[c], Liza Makowski[a,c], Jeffrey C. Rathmell[d,e], Dirk P. Dittmer[a,b], and Blossom Damania[a,b,1]

[a]Lineberger Comprehensive Cancer Center, [b]Department of Microbiology and Immunology, and [c]Department of Nutrition, Gillings School of Global Public Health, School of Medicine, University of North Carolina, Chapel Hill, NC 27599; and Departments of [d]Pharmacology and Cancer Biology and [e]Immunology, Sarah W. Stedman Nutrition and Metabolism Center, Duke University Medical Center, Durham, NC 27710

The metabolic differences between B-NHL and primary human B cells are poorly understood. Among human B-cell non-Hodgkin lymphomas (B-NHL), primary effusion lymphoma (PEL) is a unique subset that is linked to infection with Kaposi's sarcoma-associated herpesvirus (KSHV). We report that the metabolic profiles of primary B cells are significantly different from that of PEL. Compared with primary B cells, both aerobic glycolysis and fatty acid synthesis (FAS) are up-regulated in PEL and other types of nonviral B-NHL. We found that aerobic glycolysis and FAS occur in a PI3K-dependent manner and appear to be interdependent. PEL overexpress the fatty acid synthesizing enzyme, FASN, and both PEL and other B-NHL were much more sensitive to the FAS inhibitor, C75, than primary B cells. Our findings suggest that FASN may be a unique candidate for molecular targeted therapy against PEL and other B-NHL.

Kaposi sarcoma-associated herpesvirus | metabolism

Primary effusion lymphoma (PEL) is a subtype of B-cell non-Hodgkin lymphoma (B-NHL), which has a poor prognosis, with a median survival time of 6 mo (1). All PEL are infected with Kaposi sarcoma-associated herpesvirus (KSHV) and, hence, represent a tightly defined subtype of B-NHL. PEL display elevated levels of activated phosphatidylinositol 3-kinase (PI3K), AKT, and mammalian target of rapamycin (mTOR) kinases (2, 3). Our group and others have shown that KSHV viral proteins such as K1 and vGPCR can activate the PI3K/AKT/mTOR pathway in B lymphocytes and endothelial cells (4–8) and that the reliance of PEL on the PI3K/AKT/mTOR pathway can be exploited to treat PEL by using inhibitors of this pathway (2, 3). Our group has also reported that other types of nonviral B-NHL, e.g., follicular lymphomas, display activated PI3K/AKT/mTOR kinases as well (9).

The PI3K/AKT/mTOR signaling pathway is essential for the control of cell proliferation and protein translation and also regulates anabolic activities within the cell (10). PI3K/AKT signaling is known to regulate aerobic glycolysis by controlling the expression and localization of the glucose transporter GLUT1 (11) and expression of glycolytic enzymes (12). PI3K activation results in PDK1 and subsequently AKT activation, which is necessary for the induction of glycolytic enzymes (10). The ability of cancer cells to selectively induce aerobic glycolysis to generate ATP was first reported by Otto Warburg (13). Glycolysis generates fewer ATP per molecule of glucose compared with oxidative phosphorylation and produces lactate, which is excreted (Fig. 1A). Recent studies indicate that up-regulated aerobic glycolysis in cancer cells exerts a protective effect against apoptosis (14). Moreover, the requirement for high rates of macromolecular synthesis required by rapidly proliferating cancer cells is met by up-regulating glycolysis (15).

AKT also activates the mTOR signaling complex, which regulates protein translation. Under nutrient abundant conditions, mTOR activation stimulates aerobic glycolysis and de novo lipid synthesis, mediated via mobilization of the SREBP group of transcription factors (16). SREBP-1 induces the transcription of fatty acid synthase (FASN), which is a multienzyme complex responsible for synthesizing cellular lipids. FASN is expressed in the liver and present at low levels in other tissues. However, many human cancers express high levels of FASN (17, 18), and FASN is posited to be a metabolic oncogene (19). Moreover, aberrant PI3K signaling in cancer cells has been demonstrated to drive FASN expression via constitutive SREBP-1c activity (20, 21). In this work, we investigated the metabolic sequelae of PI3K/AKT/mTOR pathway activation on the metabolism of B-NHL, with a focus on PEL.

Results

PEL Display Elevated Aerobic Glycolysis. To determine the minimum glucose (Glc) requirement of PEL cells, 2×10^5 PEL cells were cultured in Glc-free media with defined amounts of D-Glc, and cell survival was monitored by using two independent techniques: trypan blue exclusion (Fig. 1B, Left) and MTS assay (Fig. 1B, Right). Viability of BCP-1, a representative PEL cell line, decreased when the D-Glc concentration in the growth medium was lowered, and the reduction in cell viability correlated with a dose-dependent decrease in Glc concentration (Fig. 1B). These data were similar in other PEL lines tested, including BC-1, BCBL-1, BCLM, and VG-1.

Next, 2×10^5 PEL cells were treated with increasing concentrations of the glycolytic inhibitor 2-deoxy-D-glucose (2DG), a D-Glc mimetic that cannot be metabolized by glycolytic enzymes, thereby inhibiting glycolysis. Cells were cultured in complete media, which contains 2 mM D-Glc, containing increasing doses of 2DG for 0, 12, or 24 h and then analyzed by MTS assay. The proliferation of BCBL-1, a representative PEL, was inhibited in a dose-responsive manner by 2DG (Fig. 1C), indicating that the inhibition of glycolysis is sufficient to reduce PEL cell viability.

Intracellular and extracellular levels of Glc and lactate were measured from primary B lymphocytes isolated from six individual healthy donors and six different PEL cell lines: BC-1, BC-3, BCBL-1, BCP-1, JSC-1, and VG-1. Averaged intensities of intracellular metabolites were normalized to total cellular protein, and extracellular metabolite intensities were normalized to the total volume of spent media. Compared with primary B cells, PEL contained lower levels of intracellular Glc and elevated levels of intracellular lactate (Fig. 2A), indicative of up-regulated glycolytic flux. Analysis of the spent growth media from equivalent numbers of cells revealed higher levels of extracellular lactate and pyruvate in the growth medium of PEL cells compared with primary B cells (Fig. 2B). PEL media had a concurrent decrease in extracellular D-Glc, confirming
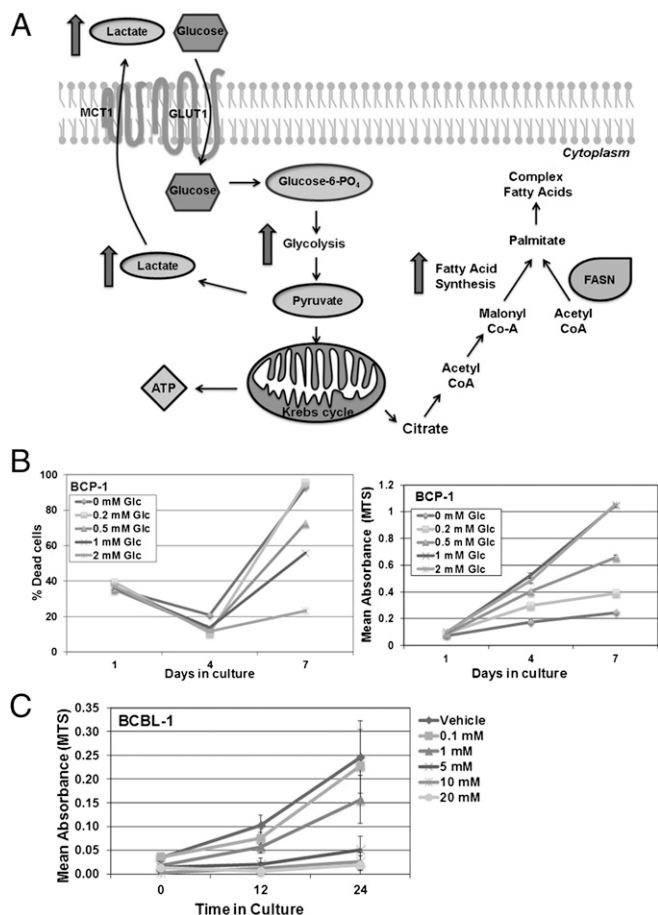
Fig. 1. Glycolysis and FAS pathways. (*A*) Once glucose (Glc) enters the cell through transporters such as GLUT1, hexokinase rapidly phosphorylates Glc into Glc-6-phosphate, which participates in glycolysis to generate 2 ATP. Pyruvate, the end product of glycolysis, is converted into lactate by lactate dehydrogenase and is secreted through monocarboxylate transporters (for e.g., MCT1). Alternatively, pyruvate can be further oxidized in the mitochondrion via the Krebs cycle to yield 36 ATP per molecule of Glc. Citrate, an intermediate metabolite, can exit the Krebs cycle and be transported into the cytoplasm, where it can be broken down into acetyl-CoA. Acetyl-CoA is converted into malonyl-CoA by acetyl-CoA carboxylase, which is the commitment step of FAS. Acetyl- and malonyl-CoA, in a series of reactions, are combined by FASN, a multienzyme polypeptide, to yield palmitate (C16), which is then elongated or desaturated into other fatty acids. These fatty acids can be used to further synthesize other macromolecules and lipids necessary for dividing cells. (*B*) BCP-1, a representative PEL, is sensitive to Glc deprivation from growth medium, which normally has 2 mM glucose. Reduction of Glc concentration in growth medium increases the percentage of dead cells, as visualized by trypan blue exclusion (*Left*) and reduces BCP-1 proliferation as determined by MTS assay (*Right*). (*C*) BCBL-1, another representative PEL, is susceptible to 2DG in a dose-dependent manner. Error bars are ± SEM, and data are representative of multiple independent experiments.

enhanced Glc uptake and increased glycolysis in PEL compared with primary B cells.

We also measured the glycolytic flux of B-NHL and primary B cells. Cells were pulsed with 10 μCi of D-[5-^{3}H](*N*)-glucose. [^{3}H]-H$_2$O generated through glycolysis was measured, and glycolytic flux was determined by normalizing counts per million to the total protein input. We first compared PEL to primary B cells and found that glycolytic flux was significantly increased ($P \leq 0.001$) up to fourfold in PEL cells compared with primary human B cells; Fig. 2*C* shows a representative panel of PEL and primary B cells. To determine whether heightened glycolysis was a common feature of other B-NHL, we compared the glycolytic fluxes
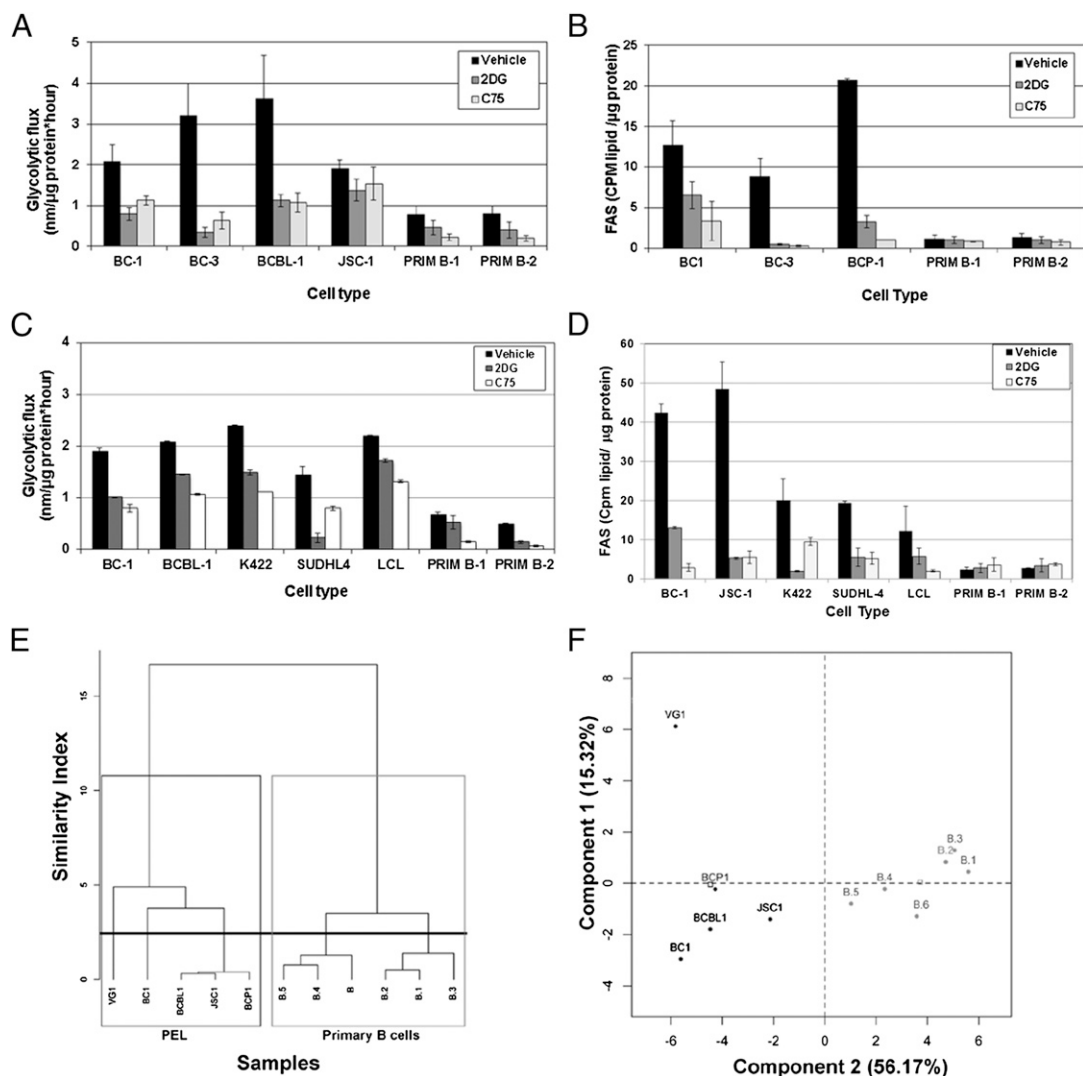
of the Burkitt lymphoma (BL) cell line CA46, and the follicular lymphoma (FL) cell lines K422 and SUDHL4, the PEL lines BC-1 and BCBL-1, and primary B cells derived from two healthy donors. Importantly, CA46, K422, and SUDHL4 are EBV- and KSHV-negative, which allow us to compare PEL to lymphomas that do not depend on viral infection. Fig. 2*D* demonstrates that all B-NHL have an elevated glycolytic flux, whereas primary B cells consistently have a lower rate of glycolysis compared with all lymphoma cell lines. These data indicate that despite distinct etiologies of each of these lymphomas, activation of the Warburg effect is a common feature among all B-NHL examined.

Up-Regulation of Fatty Acid Synthesis (FAS) in PEL. FASN is a multifunctional protein complex responsible for synthesizing all cellular fatty acids. We analyzed equivalent amounts of lysate of PEL cell lines and primary B cells by immunoblotting to compare the relative expression of FASN protein. As shown in Fig. 3*A*, FASN was highly expressed in every PEL cell line analyzed (Fig. 3*A*), whereas FASN expression was barely detectable in lysates from primary B cells. PEL and primary B cells were also stained with the lipophilic dye Nile Red and visualized by using fluorescence microscopy (Fig. S1). PEL cells contain many cytoplasmic lipid droplets that are absent in primary B cells, indicative of intracellular lipid accumulation. To determine whether FASN protein expression correlated
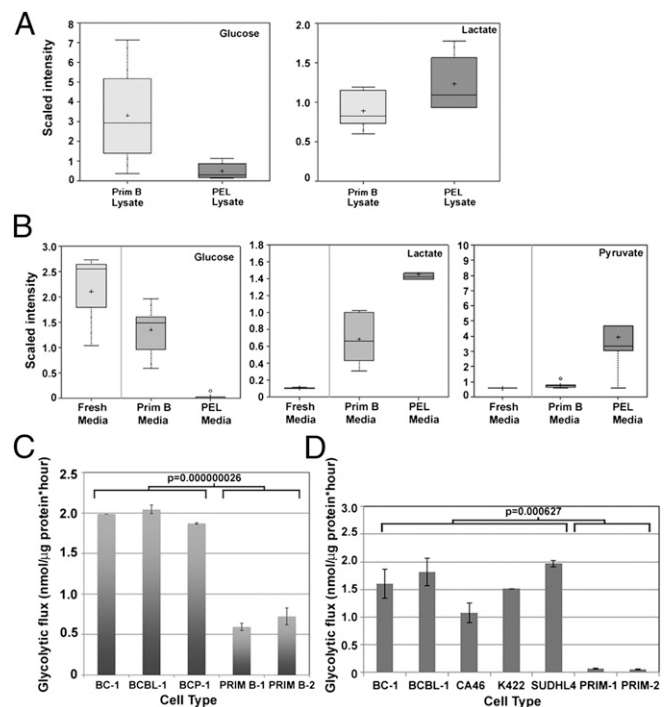
Fig. 2. PEL up-regulate glycolysis. The protein-normalized relative intensities ("scaled intensities") of intra- and extracellular concentrations of glycolytic intermediates, represented as box and whisker plots, are significantly different between PEL and primary B cells. Data are the combined average of six different primary B cells derived from six healthy donors and six PEL lines. (*A*) Intracellular levels of free Glc are lower, whereas that of lactate are higher in PEL, compared with primary B cells. (*B*) The spent media of PEL contains lower concentration of Glc and increased levels of lactate and pyruvate compared with the spent media of primary B cells. (*C*) Equal numbers of PEL and primary cells were cultured for 24 h, and glycolytic flux was measured. PEL cells exhibit significantly increased ($P = 0.000000026$) glycolysis compared with primary human B cells. (*D*) Equal numbers of PEL, BL (CA46), FL (K422 and SUDHL4), and primary B cells were cultured for 24 h, and glycolytic flux was measured. All B-NHL have significantly ($P = 0.000627$) higher glycolytic flux compared with primary B cells. Data are normalized to total input protein. Error bars are ± SEM; data are one representative of more than five independent experiments.

Fig. 3. FAS is a critical and essential metabolic pathway for the proliferation of PEL. (*A*) PEL express higher levels of FASN compared with primary B cells. Ku80 is shown as a loading control. (*B*) The rate of FAS in PEL is significantly higher ($P = 0.012$) compared with primary B cells. (*C*) PEL (BC-1 and BCBL-1) have higher FAS rates compared with BL (CA46) and FL (K422 and SUDHL4). Collectively, all B-NHL have a higher FAS rate compared with primary B cells. Data are normalized to total input protein and is one representative of multiple independent experiments. Error bars are ± SEM. (*D*) Inhibition of FAS using varying concentrations of the FASN inhibitor, C75, leads to a dose-dependent increase in cell death in BC-1 (*Left*) and BC-3 (*Right*) PEL cells, as measured by trypan blue exclusion. (*E*) Inhibition of FAS using C75 leads to minimal cell death in primary B cells from two donors, as measured by trypan blue exclusion. Error bars are ± SEM.

with activation of FAS, we determined the rate at which de novo FAS occurs in PEL and primary B cells by measuring the degree of incorporation of radiolabeled Glc into the cellular lipid fraction. Radioactive counts from the extracted lipid fraction of each cell type were normalized to the total protein content of the cell pellet. We found that PEL synthesize fatty acids from Glc at a substantially higher rate ($P = 0.012$) compared with primary cells (Fig. 3*B*). Our findings extend to other B-NHL, because similar to PEL, the FAS rates of CA46, K422, and SUDHL4 were significantly ($P = 0.02$) higher than primary B cells (Fig. 3*C*).

Increased levels of lipid in PEL compared with primary B cells could be a consequence of either reduced catabolism of lipids or increased FAS. We therefore measured the rate of fatty acid oxidation (FAO). Fig. S2 demonstrates that FAO rates are not significantly different between PEL and primary B cells. Thus,

FAS seems to be the dominant fatty acid metabolic pathway up-regulated in PEL.

To establish the importance of increased FAS for B-NHL survival, we inhibited FAS with C75, a FASN inhibitor (22). When treated with increasing doses of C75, all B-NHL cells displayed a dose-dependent increase in cell death, as measured by trypan blue exclusion. In Fig. 3*D*, BC-1 and BC-3 are shown as representative PEL. Fig. S3 *A* and *B* respectively demonstrate that both CA46 and SUDHL4 are susceptible to C75, however, the degree of susceptibility is not as great as that of PEL. FAS inhibition by C75 resulted in activation of proapoptotic caspase-3 in all B-NHL (Fig. S3*C*). In contrast, primary B cells were minimally affected by C75 (Fig. 3*E*). Thus, the susceptibility of these B-NHL lines to C75, while sparing primary B cells, reveals FAS as a unique target for molecular targeted therapy in B-NHL.

B lymphocytes isolated from the peripheral blood are normally in a resting state. PEL are lymphoma cells and, hence, proliferate continuously in the absence of specific stimulus. To rule out the possibility that differentials in glycolysis and FAS were a consequence of proliferation rather than the transformed phenotype, we measured glycolytic flux, FAS rates, and FASN expression in activated primary B cells. Primary B cells were treated for 48 h with either PBS as vehicle or 10 μg/mL lipopolysaccharide (LPS) to stimulate B-cell proliferation as reported (23), after which proliferation was confirmed by using the MTS assay (Fig. 4*A*), and live cell counts were measured by trypan blue exclusion (Fig. S4*C*). The rates of glycolysis (Fig. 4*B*) and lipid synthesis (Fig. 4*C*) were quantified and compared with PEL (BC-1 and BCBL-1). LPS-stimulated B cells proliferated more than unstimulated B cells, as expected (Fig. 4*A* and Fig. S4*C, Right*). Despite the elevated glycolytic rate of stimulated primary B cells, their rate of glycolysis was still significantly lower ($P \leq 0.01$) than that of vehicle-treated PEL cells (Fig. 4*B*). Interestingly, FAS did not substantially change in LPS-stimulated versus vehicle-treated primary B cells (Fig. 4*C*). However, both these rates of FAS were significantly lower than that of an equivalent number of vehicle-treated BC-1 and BCBL-1 PEL cells ($P \leq 0.05$). LPS stimulation of PEL did not further increase glycolysis or FAS compared with vehicle-treated PEL (Fig. S4 *A* and *B*), and PEL proliferation was not altered by LPS treatment, unlike primary B cells that did

Fig. 4. LPS-driven proliferation of primary B cells is not linked to the rate of FAS as is evident in untreated PEL. (*A*) Stimulation of primary B cells with 10 μg/mL LPS leads to an increase in proliferation as measured by MTS assay. (*B*) Glycolysis is minimally up-regulated in LPS-stimulated proliferating primary B cells, but the rates are significantly lower (*$P \leq 0.05$) than those of vehicle-treated PEL. (*C*) FAS is not up-regulated in LPS-stimulated primary B cells and the rates of FAS are significantly lower (*$P \leq 0.01$) than those seen in untreated PEL. Error bars are ± SEM. (*D*) There is a slight increase in FASN expression in LPS-stimulated proliferating primary B cells, but these levels are 5 times lower than that seen in untreated PEL (quantified using densitometry). Ku80 is a loading control.

Fig. 5. Glycolysis and FAS are intimately linked in B-NHL. (*A*) PEL and primary B cells treated for 72 h with 10 μg/mL C75 show a significant decrease in glycolysis ($P \leq 0.05$ for all comparisons), similar to 1 mM 2DG-treated cells (positive control). Error bars are ± SEM. (*B*) PEL cells treated for 72 h with 1 mM 2DG have decreased FAS ($P \leq 0.05$), and with 10 μg/mL C75 (positive control) have significantly decreased FAS ($P \leq 0.05$). Primary B cells display minimal FAS activity, which is not down-regulated with inhibitors. Error bars are ± SEM; data are representative of more than three independent experiments. (*C*) B-NHL (including PEL), LCL, and primary B cells treated for 72 h with 10 μg/mL C75 show a reduction in glycolysis comparable with 2DG-treated cells. (*D*) Glycolysis inhibition of B-NHL (including PEL) and LCL with 2DG substantially reduces FAS to a rate similar to the FASN inhibitor C75, but does not impact FAS in primary B cells. (*E* and *F*) A dendrogram of hierarchical clustering (*E*) and principal component analysis (*F*) of relative intensities of metabolic intermediates of glycolysis and FAS demonstrates that PEL and primary B cells display distinct metabolic profiles.

proliferate in response to LPS stimulation (Fig. S4C, *Left*). Furthermore, immunoblot analysis of cell lysates revealed that FASN expression in primary B cells was slightly increased upon LPS stimulation (Fig. 4*D*), which was still fivefold lower than that of unstimulated (vehicle-treated) PEL cells. These data potentially suggest that FASN activity is an independent phenotype of PEL rather than a consequence of increased proliferation index and that up-regulated lipid synthesis is a metabolic signature of PEL.

PEL Have a Distinct Lipid Synthesis Profile Compared with Primary B Cells. We identified the major classes of lipids resulting from FAS by culturing primary B and PEL cells in medium supplemented with D-[U-^{14}C$_6$]-Glc (24). Table S1 demonstrates that PEL and primary B cells have different amounts of de novo synthesized lipids that are derived from Glc. We found that the major components of eukaryotic cell walls, e.g., phosphatidylcholine and phosphatidylethanolamine, are preferentially and abundantly synthesized by PEL compared to primary B cells. The ratio of de novo lipids and triglycerides synthesized by using glucose precursors is much higher in PEL compared with primary B cells.

Glycolysis and FAS Are Intimately Linked in B-NHL. We measured both glycolytic flux and rates of FAS in an equivalent number of both PEL and primary B cells, in the presence of 1 mM 2DG (glycolysis inhibitor), or 10 μg/mL C75 (FASN inhibitor) for 72 h. As shown in Fig. 5*A*, 2DG inhibited glycolysis in both cell

types, as expected. However, C75 also reduced glycolysis to levels similar to that seen after 2DG treatment (Fig. 5*A*). In the converse experiment, Fig. 5*B* demonstrates that while C75 expectedly and potently inhibits FAS, 2DG also reduced FAS in PEL, suggesting that upregulated glycolysis is a mechanism for generating intermediates for fatty acid synthesis (15, 25). In contrast, the rate of FAS in primary B cells remained static and independent of 2DG treatment (Fig. 5*B*). In PEL, inhibition of FAS decreased the rate of glycoysis and conversely, glycolysis inhibition blocked FAS, demonstrating that both glycolysis and FAS are intimately linked, with inhibition of one pathway impacting the other. Moreover, these two pathways are linked in other B-NHL subsets as well. Fig. 5*C* demonstrates that FAS inhibition reduces glycolytic flux in the FL cell lines, K422 and SUDHL4, and an EBV-positive lymphoblastoid cell line (LCL). Conversely, Fig. 5*D* indicates that glycolysis inhibition potently reduces FAS in the B-NHL and LCL lines.

Thirty-nine glycolysis and FAS intermediates (listed in Table S2) from five PEL cell lines and six primary B-cell samples were analyzed, and the data were subjected to unsupervised clustering (Fig. 5*E*) and principal component analysis (PCA) (Fig. 5*F*). PEL and primary B cells clearly segregated into two distinct groups as represented in the dendrogram (Fig. 5*E*) or along component 2 in the PCA (Fig. 5*F*). The dissimilarity between the PEL cluster and the primary B-cell cluster was much greater than among primary B-cell cultures alone or among the PEL alone.

MICROBIOLOGY
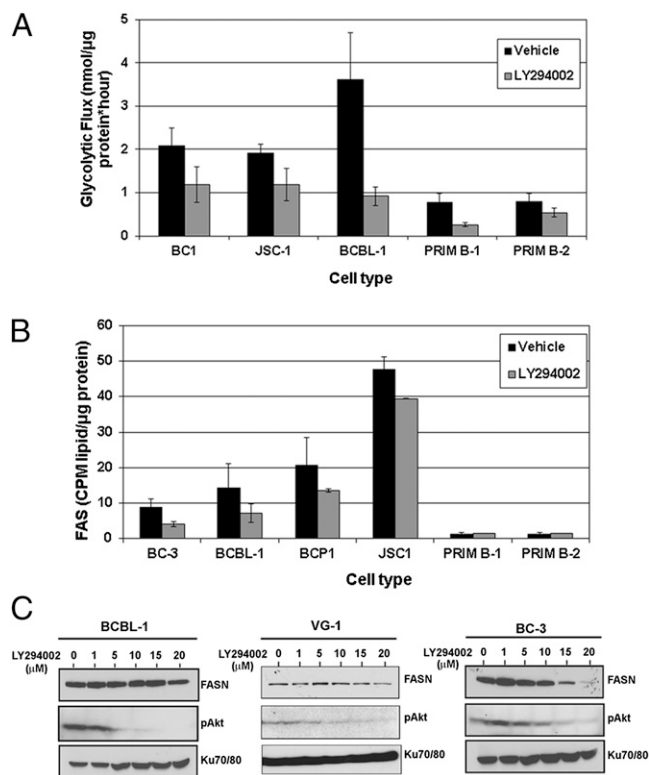
Fig. 6. PI3K inhibition decreases FAS and glycolysis in PEL cells. (*A*) Treatment of cells for 72 h with a noncytotoxic dose (1 μM) of LY294002 reduces the rate of glycolysis in both PEL ($P \leq 0.01$) and primary B cells ($P \leq 0.01$). Error bars are ± SEM. (*B*) LY294002 treatment significantly reduces FAS in PEL ($P \leq 0.01$) but does not alter the already low rate of FAS in primary B cells. Error bars are ± SEM. (*C*) Treatment with LY294002 leads to a dose-dependent decrease in expression of FASN in BCBL-1 (*Left*), BC-3 (*Right*), and VG-1 (*Center*) PEL cells, with a concurrent decrease in pAKT.

PI3K/AKT Is Required for Increased Glycolysis and FAS in PEL. PI3K/AKT signaling is known to regulate glycolysis, and a previous report indicated that PI3K inhibition reduces glycolytic flux and induces cell cycle arrest in diffuse large B-cell lymphomas (26). We investigated whether inhibiting PI3K using LY294002 would alter glycolysis and FAS in PEL. We first determined a dose of LY294002 (1 μM) that was not significantly cytotoxic to PEL cell lines over the course of 72 h (Fig. S5). Equivalent numbers of PEL and primary B cells were treated with either 1 μM LY294002 or DMSO for 72 h, after which the rates of glycolysis and FAS were measured as described above. As expected, LY294002 dramatically ($P \leq 0.01$) reduced the glycolytic flux in both PEL and primary B cells (Fig. 6*A*). We also found that LY294002 significantly ($P \leq 0.01$) decreased the rates at which PEL cells incorporated radiolabeled Glc into lipids via FAS (Fig. 6*B*). However, primary B cells were unaffected (Fig. 6*B*). Moreover, as shown in Fig. 6*C*, LY294002 treatment resulted in a dose-dependent reduction of FASN expression in PEL, providing a potential mechanism for the dramatic reduction in FAS in PEL upon PI3K inhibition. Collectively, these data indicate that not only does PI3K/AKT inhibition in PEL decrease FASN expression, but it also diminishes glycolytic flux, thereby preventing Glc incorporation into newly synthesized fatty acids.

FAS Inhibition Leads to an Accumulation of Carnitine. The overall levels of free carnitine are lower in PEL compared with primary B cells (Fig. S6*A*). All data are normalized to protein content and are shown in Fig. S6. Lowered carnitine levels in colon cancer cells have been shown to inhibit the generation of apoptosis-inducing O_2^- radicals (27). Treatment of PEL and primary

B cells with the FAS inhibitor, C75, resulted in a decrease in cellular-free carnitine in both cell types; however, the magnitude of reduction was greater in PEL (31% reduction) compared with primary B cells (13.5% reduction), which might reflect the fact that PEL are more sensitive to C75 than primary B cells.

We also measured the relative levels of distinct acyl-carnitine intermediates by MS. We found that many of the even-chained acyl-carnitines were increased in PEL compared with primary B cells (Fig. S6 *B and C*), which may indicate incomplete oxidation of fatty acids (28). In contrast, primary B cells display higher amounts of C3 and C5 acyl-carnitines, which may suggest a reliance on oxidation of amino acids rather than fatty acids (28).

Combination of LY294002 and C75 Is Most Effective at Inhibiting PEL Proliferation. Overall, our findings suggest that FAS is up-regulated in PEL and other B-NHL. The above experiments indicate that the PI3K inhibitor, LY294002, blocks glycolysis and FAS in PEL (Fig. 6). Therefore, we sought to determine whether a combination of LY294002 and C75 would enhance PEL cell death. We treated PEL cells with increasing doses of LY294002 and C75 for 72 h and measured cell survival by trypan blue exclusion. As seen in Fig. S7, either drug alone reduced cell viability in a dose-dependent manner. However, combined treatment with 10 μM LY294002 and 10 μg/mL C75 led to death of ~75% of PEL cells ($P \leq 0.05$) in culture. These data confirm that FAS inhibition may be an efficacious treatment modality for PEL and could be combined with existing PI3K-targeted chemotherapeutics.

Discussion

We report that B-NHL demonstrate activation of the Warburg effect, evident in their increased glycolytic activity, even under normoxic culture conditions. In this paper, we focused on PEL as a subset of B-NHL. In particular, KSHV-infected PEL are highly sensitive to Glc withdrawal and the glycolysis inhibitor, 2DG. Lactate, a byproduct of glycolysis, is present in high levels in the growth media of PEL. Our flux measurements confirm up-regulated rates of glycolysis in all B-NHL cells examined, including PEL, compared with primary B cells from healthy donors. Additionally, KSHV infection of endothelial cells was previously reported to increase glycolysis (29).

We also found that B-NHL actively synthesize fatty acids from glucose. Enhanced FAS in PEL can at least partly be attributed to the overexpression of FASN, whereas FASN expression or biosynthetic activity in human primary B cells was barely detectable. These data suggest that aberrant FAS activation may be a metabolic adaptation of PEL and B-NHL. We report that FAS inhibition by C75 reduced the viability of B-NHL, whereas primary B cells remain largely unaffected. Moreover, C75 also sensitized PEL cells to the PI3K inhibitor LY294002. Susceptibility to FAS inhibition may arise due to oncogene addiction, a phenomenon where cancer cells are highly sensitive to inactivation of a pathway that they depend upon for survival and proliferation (30). Our data indicate that up-regulated FAS is a characteristic shared by B-NHL of differing etiologies, and this exquisite dependence on FAS presents an opportunity to use molecular targeted therapy selectively against B-NHL, while sparing primary B cells.

Elevated FAS in PEL contributes to an abundance of de novo synthesized, Glc-derived triglycerides and phospholipids, suggesting that newly generated fatty acids are rapidly incorporated into membrane lipids and triglyceride stores to accommodate the dramatic proliferative rates of lymphoma cells. It is important to note that FAS precursors can also be generated by other biochemical pathways such as glutamine metabolism. However, their relevance in the context of B-NHL remains to be determined.

We report that glycolysis and FAS are intertwined in PEL and other B-NHL because inhibition of glycolysis affected FAS and vice versa. The fact that inhibition of glycolysis causes a reduction in FAS suggests that glycolysis fuels the synthesis of fatty acids in PEL and B-NHL by providing acetyl-coA intermediates. Conversely, FAS inhibition may result in decreased glycolysis, if there

is a feedback loop within the cells whereby decreased FASN biosynthetic activity leads to a decrease in the generation of glycolytic intermediates required to fuel FAS.

Fatty acids are essential for subsequent synthesis of macromolecules and cell membranes, both of which are necessary for rapidly dividing cancer cells. Interestingly, primary B cells stimulated to proliferate with LPS up-regulated glycolysis, along with a concurrent expression of FASN; however, in proliferating primary B cells, the rate of neither pathway was comparable to the high degree of glycolysis and FAS taking place in untreated PEL. These data suggest that enhanced FAS and up-regulated FASN expression is an advantageous metabolic adaptation of PEL and other B-NHL. PI3K/AKT pathway activation in PEL contributes to the increase in both glycolysis and FAS, because treatment of PEL with a noncytotoxic dose of the PI3K inhibitor, LY294002, reduced the rate of glycolysis and FASN expression, thus diminishing the rate of FAS. However, in primary B cells, LY294002 decreased glycolytic flux, but did not appear to affect the rate of FAS.

Collectively, our data suggest that hyperactivated FAS is essential for the growth advantage of B-NHL. Further, these data indicate that targeting FASN may be an efficacious therapeutic strategy for B-NHL.

Materials and Methods

Detailed methods and supporting figures are available in *SI Materials and Methods*.

Cell Isolation and Culture. Primary B cells were isolated by negative selection from donor buffy coats using the B-cell isolation kit II (Miltenyi). Cell lines were cultured in identical media and culture conditions as described (9, 31, 32).

Cell Viability Assays and Immunoblotting. Proliferation was measured by using the Cell Titer 96AQueous One Solution (Promega), and apoptosis was measured by using the ApoAlert Caspase-3 assay (Clontech). Immunoblotting was performed as described (3).

Measurement of Glycolytic Flux, Lipid Synthesis, and Analysis of Newly Synthesized Lipids. Glycolytic flux (33) and lipid synthesis (34) were measured as described. Analysis of lipid components was performed by using described methods (24). All data were analyzed by using a two-tailed type II Student's *t* test for significance; *P* values are indicated at appropriate locations within figure legends.

Metabolic Profiling. Metabolic profiling, peak identification, and curation was performed by Metabolon using described methods (35).

Bioinformatics. Hierarchical clustering and principal component analysis was conducted by using the R programming environment (version 2.13.2) package FactoMineR.

1. Boulanger E, et al. (2005) Prognostic factors and outcome of human herpesvirus 8-associated primary effusion lymphoma in patients with AIDS. *J Clin Oncol* 23: 4372–4380.
2. Sin SH, et al. (2007) Rapamycin is efficacious against primary effusion lymphoma (PEL) cell lines in vivo by inhibiting autocrine signaling. *Blood* 109:2165–2173.
3. Bhatt AP, et al. (2010) Dual inhibition of PI3K and mTOR inhibits autocrine and paracrine proliferative loops in PI3K/Akt/mTOR-addicted lymphomas. *Blood* 115: 4455–4463.
4. Wang L, et al. (2004) The Kaposi's sarcoma-associated herpesvirus (KSHV/HHV-8) K1 protein induces expression of angiogenic and invasion factors. *Cancer Res* 64: 2774–2781.
5. Tomlinson CC, Damania B (2004) The K1 protein of Kaposi's sarcoma-associated herpesvirus activates the Akt signaling pathway. *J Virol* 78:1918–1927.
6. Wang L, Dittmer DP, Tomlinson CC, Fakhari FD, Damania B (2006) Immortalization of primary endothelial cells by the K1 protein of Kaposi's sarcoma-associated herpesvirus. *Cancer Res* 66:3658–3666.
7. Sodhi A, et al. (2004) Akt plays a central role in sarcomagenesis induced by Kaposi's sarcoma herpesvirus-encoded G protein-coupled receptor. *Proc Natl Acad Sci USA* 101:4821–4826.
8. Bais C, et al. (2003) Kaposi's sarcoma associated herpesvirus G protein-coupled receptor immortalizes human endothelial cells by activation of the VEGF receptor-2/KDR. *Cancer Cell* 3:131–143.
9. Bhende PM, Park SI, Lim MS, Dittmer DP, Damania B (2010) The dual PI3K/mTOR inhibitor, NVP-BEZ235, is efficacious against follicular lymphoma. *Leukemia* 24: 1781–1784.
10. Manning BD, Cantley LC (2007) AKT/PKB signaling: Navigating downstream. *Cell* 129: 1261–1274.
11. Wieman HL, Wofford JA, Rathmell JC (2007) Cytokine stimulation promotes glucose uptake via phosphatidylinositol-3 kinase/Akt regulation of Glut1 activity and trafficking. *Mol Biol Cell* 18:1437–1446.
12. Elstrom RL, et al. (2004) Akt stimulates aerobic glycolysis in cancer cells. *Cancer Res* 64: 3892–3899.
13. Warburg O (1956) On respiratory impairment in cancer cells. *Science* 124:269–270.
14. Hsu PP, Sabatini DM (2008) Cancer cell metabolism: Warburg and beyond. *Cell* 134: 703–707.
15. Young CD, Anderson SM (2008) Sugar and fat - that's where it's at: Metabolic changes in tumors. *Breast Cancer Res* 10:202.
16. Düvel K, et al. (2010) Activation of a metabolic gene regulatory network downstream of mTOR complex 1. *Mol Cell* 39:171–183.
17. Kuhajda FP (2000) Fatty-acid synthase and human cancer: New perspectives on its role in tumor biology. *Nutrition* 16:202–208.
18. Vazquez-Martin A, Colomer R, Brunet J, Lupu R, Menendez JA (2008) Overexpression of fatty acid synthase gene activates HER1/HER2 tyrosine kinase receptors in human breast epithelial cells. *Cell Prolif* 41:59–85.
19. Flavin R, Peluso S, Nguyen PL, Loda M (2010) Fatty acid synthase as a potential therapeutic target in cancer. *Future Oncol* 6:551–562.
20. Yoon S, et al. (2007) Up-regulation of acetyl-CoA carboxylase alpha and fatty acid synthase by human epidermal growth factor receptor 2 at the translational level in breast cancer cells. *J Biol Chem* 282:26122–26131.
21. Yang YA, Han WF, Morin PJ, Chrest FJ, Pizer ES (2002) Activation of fatty acid synthesis during neoplastic transformation: Role of mitogen-activated protein kinase and phosphatidylinositol 3-kinase. *Exp Cell Res* 279:80–90.
22. Kuhajda FP, et al. (2000) Synthesis and antitumor activity of an inhibitor of fatty acid synthase. *Proc Natl Acad Sci USA* 97:3450–3454.
23. Armerding D, Sachs DH, Katz DH (1974) Activation of T and B lymphocytes in vitro. III. Presence of Ia determinants on allogeneic effect factor. *J Exp Med* 140:1717–1722.
24. Teng YW, Mehedint MG, Garrow TA, Zeisel SH (2011) Deletion of betaine-homocysteine S-methyltransferase in mice perturbs choline and 1-carbon metabolism, resulting in fatty liver and hepatocellular carcinomas. *J Biol Chem* 286:36258–36267.
25. Vander Heiden MG, Cantley LC, Thompson CB (2009) Understanding the Warburg effect: The metabolic requirements of cell proliferation. *Science* 324:1029–1033.
26. Faber AC, et al. (2006) Inhibition of phosphatidylinositol 3-kinase-mediated glucose metabolism coincides with resveratrol-induced cell cycle arrest in human diffuse large B-cell lymphomas. *Biochem Pharmacol* 72:1246–1256.
27. Wenzel U, Nickel A, Daniel H (2005) Increased carnitine-dependent fatty acid uptake into mitochondria of human colon cancer cells induces apoptosis. *J Nutr* 135:1510–1514.
28. Newgard CB, et al. (2009) A branched-chain amino acid-related metabolic signature that differentiates obese and lean humans and contributes to insulin resistance. *Cell Metab* 9:311–326.
29. Delgado T, et al. (2010) Induction of the Warburg effect by Kaposi's sarcoma herpesvirus is required for the maintenance of latently infected endothelial cells. *Proc Natl Acad Sci USA* 107:10696–10701.
30. Weinstein IB, Joe AK (2006) Mechanisms of disease: Oncogene addiction—a rationale for molecular targeting in cancer therapy. *Nat Clin Pract Oncol* 3:448–457.
31. Roy D, Dittmer DP (2011) Phosphatase and tensin homolog on chromosome 10 is phosphorylated in primary effusion lymphoma and Kaposi's sarcoma. *Am J Pathol* 179:2108–2119.
32. Roskrow MA, et al. (1998) Epstein-Barr virus (EBV)-specific cytotoxic T lymphocytes for the treatment of patients with EBV-positive relapsed Hodgkin's disease. *Blood* 91: 2925–2934.
33. Rathmell JC, Farkash EA, Gao W, Thompson CB (2001) IL-7 enhances the survival and maintains the size of naive T cells. *J Immunol* 167:6869–6876.
34. Deberardinis RJ, Lum JJ, Thompson CB (2006) Phosphatidylinositol 3-kinase-dependent modulation of carnitine palmitoyltransferase 1A expression regulates lipid metabolism during hematopoietic cell growth. *J Biol Chem* 281:37372–37380.
35. Reitman ZJ, et al. (2011) Profiling the effects of isocitrate dehydrogenase 1 and 2 mutations on the cellular metabolome. *Proc Natl Acad Sci USA* 108: 3270–3275.

MICROBIOLOGY